Eur Biophys J (2002) 31: 317–322
DOI 10.1007/s00249-002-0232-4

BIOPHYSICS LETTER

Manuela Menke · Stephanie Künneke · Andreas Janshoff

Lateral organization of G_{M1} in phase-separated monolayers visualized by scanning force microscopy

Received: 14 January 2002 / Revised: 28 March 2002 / Accepted: 4 April 2002 / Published online: 14 June 2002

Abstract Phase separation of glycolipids in lipid mono- and bilayers is of great interest for the understanding of membrane function. The distribution of the ganglioside G_{M1} in sphingomyelin (SM)/1-palmitoyl-2-oleoyl-*sn*-glycero-3-phosphocholine (POPC), SM/1,2-dipalmitoyl-*sn*-glycero-3-phosphocholine (DOPC) and SM/cholesterol/POPC Langmuir-Blodgett (LB) monolayers transferred at 36 mN/m has been studied by scanning force microscopy. Besides lateral organization of the glycolipid in LB monolayers as deduced from topography, material properties have been investigated by phase imaging, pulsed force mode and force modulation microscopy. It was shown that G_{M1} preferentially clusters in an ordered lipid matrix, i.e. the SM phase in the case of the SM/POPC and SM/DOPC mixture or in the ordered phase of POPC/SM/cholesterol monolayers. At higher local concentrations, three-dimensional protrusions enriched in G_{M1} occur, which may represent a precursor for the formation of micelles budding into the aqueous subphase. Electronic supplementary material to this paper can be obtained by using the Springer Link server located at http://dx.doi.org/10.1007/s00249-002-0232-4.

Keywords Glycolipids · Gangliosides · Monolayers · Membranes · Scanning force microscopy

Introduction

The lateral distribution of receptors in lipid bilayers is of pivotal interest for the understanding of ligand-receptor interactions at the cellular membrane, the structure-function relationship of endocytosis, membrane trafficking and signal transduction. In particular, gangliosides, negatively charged ceramide-based glycolipids bearing at least one sialic residue, have been recognized as important receptor lipids for bacterial toxins, lectins, initial docking of virus capsids and also as modulating compounds for other receptors such as the insulin receptor and integrins, which are responsible for cell-substrate interaction (Fishman and Brady 1976; Habermann and Dreyer 1986; Hakomori 1981; Holmgren et al. 1980; Janshoff et al. 1996, 1997; Singh et al. 2000; Tamm et al. 1996). For instance, the monosialoganglioside G_{M1} is known to be the natural receptor for cholera toxin. Despite their abundance, little is known about the lateral structural organization of glycolipids in the outer leaflet of the biological membrane. An increasing amount of convincing evidence has been collected that points towards the formation of ordered microdomains in the outer leaflets of cellular membranes that are enriched in sphingolipids and cholesterol, thus providing the prerequisite for the organization and clustering of receptor molecules within the membrane (Brown and London 1998a, 1998b, 2000; Dietrich et al. 2001; Vyas et al. 2001). Treatment of the plasma membrane with detergents results in the formation of a detergent-resistant network referred to as DIGs – detergent insoluble membrane fractions (Brown and London 2000; Fivaz et al. 2000; Simons and Ikonen 1997). These submicron domains, rafts, display physical properties which can be identified with the liquid ordered phase (l_o phase). The l_o phase is an intermediate between the gel phase and the liquid disordered phase, showing significant higher lateral mobility than lipids in the gel phase along with more ordered chains (Brown and London 2000).

Model membranes of different kinds such as liposomes, solid-supported bilayers and monolayers at the air-water interface have been used throughout the literature to investigate phase separation phenomena, avoiding the state of complexity met in biological membranes. Although the organization of gangliosides in model membranes has been extensively studied by a

Electronic supplementary material to this paper can be obtained by using the Springer Link server located at http://dx.doi.org/10.1007/s00249-002-0232-4

M. Menke · S. Künneke · A. Janshoff (✉)
Institut für Physikalische Chemie,
Welder Weg 11, Johannes Gutenberg-Universität,
55099 Mainz, Germany
E-mail: janshoff@mail.uni.mainz.de
Tel.: +49-6131-3923930
Fax: +49-6131-3922970

variety of different techniques, there is still lack of consistency, which may partly be attributed to a different scale, i.e. spatial resolution, labeling techniques, interference from probes and preparation of the membranes (Yuan and Johnston 2000 and references therein). Recently, scanning probe techniques have added a significant amount of invaluable information about phase separation in mono- as well as bilayers systems (Dufrene and Lee 2000; Ross et al. 2001; Yuan and Johnston 2000, 2001). For instance, Le Grimellec and co-workers performed a thorough study on the domain formation of various monolayers consisting of sphingomyelin (SM), cholesterol and 1-palmitoyl-2-oleoyl-*sn*-glycero-3-phosphocholine (POPC), modeling the outer leaflet of the renal brush border membrane (Milhiet et al. 2001). The authors found phase separation in the POPC/SM monolayers (liquid expanded/liquid condensed, LE/LC) up to a content of 33 mol% cholesterol. The persistent lateral heterogeneity is probably due to the preferential interaction of cholesterol with SM, as pointed out by Slotte (1999).

Vie et al. (1998) showed that ganglioside G_{M1} is enriched in the liquid condensed phase of mixed monolayer films of DPPC and DOPC. Further confirmation that gangliosides preferentially distribute in the ordered phase has been provided recently by Yuan and Johnston (2000). The authors observed clustering of G_{M1} in the center of the LC phase and at the boundary of the LC domains. G_{M1}-enriched domains could be identified by an increased height due to the bulky headgroup of G_{M1} and clustering was attributed to weak carbohydrate interactions. In contrast, Mou et al. (1995) found no segregation of G_{M1} in phosphatidylcholine bilayers by scanning force microscopy (SFM) using cholera toxin as a label.

In this paper we investigate, for the first time, phase separation and material properties of mixed monolayers of SM, cholesterol and POPC or DOPC supplemented with a low content of G_{M1} (0.2 mol%) by means of SFM, providing high-resolution spatial information about topography, elasticity and adhesion on a nanometer scale. The study provides convincing evidence, by combining topography information with phase imaging and force modulation microscopy, that G_{M1} is indeed preferentially distributed in more ordered membrane regions such as the SM-enriched phase, but also forms domains enriched in G_{M1} within the ordered matrix itself. Furthermore, we found evidence for the formation of G_{M1}-enriched micelles budding into the water subphase, as predicted by McConnell (Radhakrishnan and McConnell 2000).

Materials and methods

Materials

POPC, DOPC and SM from brain were purchased from Avanti Polar Lipids (Alabaster, Ala., USA) and used without further purification. 45.5% of the SM consists of 18:0 fatty acids, 23.3% of 24:0, 7.2% of 22:0, 5.1% of 20:0, 1.7% of 16:0 and 6.3% were unsaturated 24:1 chains. Cholesterol, chloroform, ganglioside G_{M1} and methanol were purchased from Sigma-Aldrich (Dreieich, Germany).

Film balance measurements

Surface pressure-area isotherms were obtained at 20 °C on a Wilhelmy balance (Riegler and Kirstein, Golm, Germany) with an operational area of 144 cm^2. Lipid monolayers were spread on a subphase containing ultrapure water. The organic solvent was allowed to evaporate for 10 min before the film was compressed at a rate of 2.8 cm^2/min. For the preparation of Langmuir-Blodgett (LB) films a Wilhelmy balance equipped with a 25 ml Teflon trough (15.4 cm×2.5 cm) and a dipper device was used. LB films for SFM measurements were deposited on freshly cleaved mica sheets. After 10 min, the monolayer was compressed to a surface pressure of 36 mN/m at a rate of 1.79 cm^2/min and equilibrated for 30 min. The lipid film was deposited onto the substrate with a pulling speed of 0.7 mm/min while maintaining the surface pressure to a constant value of 36 mN/m.

Scanning force microscopy

Surface images of the LB monolayers were obtained using a Nanoscope IIIa (Bioscope) scanning force microscope (Digital Instruments, Santa Barbara, Calif., USA) operating in contact mode, tapping mode, force modulation (FM, Jourdan et al. 1999) and pulsed force mode (PFM, WiTec, Ulm, Germany) (Magonov et al. 1997; Rosa-Zeiser et al. 1997). Microfabricated silicon nitride tips (NP-S, Digital Instruments) with an approximate tip radius of 5–20 nm and a nominal spring constant of 0.06–0.56 N/m were used as purchased for force modulation, pulsed force and contact mode microscopy. For tapping mode measurements, silicon tips with an approximate resonant frequency of 300 kHz and an approximate force constant of 48 N/m were purchased from Nanosensors (Wetzlar-Blankenfeld, Germany).

Results and discussion

The motivation for investigating LB monolayers composed of DOPC/SM (80:20) or POPC/SM (80:20) is based on the fact that most plasma membranes exhibit 10–20 mol% SM, in which most of the lipid is located in the outer leaflet. According to Brown and London (2000), a lipid composition of POPC/Chol/SM of 2:1:1 should result in coexistence of the liquid disordered and the liquid ordered phases. This way we can decide if G_{M1} is preferentially distributed in an ordered or a disordered matrix.

Monolayers composed of DOPC/SM (80:20) or POPC/SM (80:20) transferred to mica at 36 mN/m display typical phase separation, in which the higher phase (lighter) consists of SM in the LC phase and the lower phase of DOPC is in the LE phase up to collapse of the monolayer at high pressure. Figure 1A shows a representative SFM image (topography) obtained from tapping-mode imaging of a LB monolayer of DOPC/SM (80:20), while Fig. 1B shows the phase information, revealing that the higher regions corresponding to the SM phase exhibit a larger phase shift. This might be interpreted as a higher elastic modulus for the SM domains. This is inferred from the chosen setpoint (A_{set}/A_{free} between 0.4 and 0.75), indicative of moderate tapping, which provides image contrast mainly based on

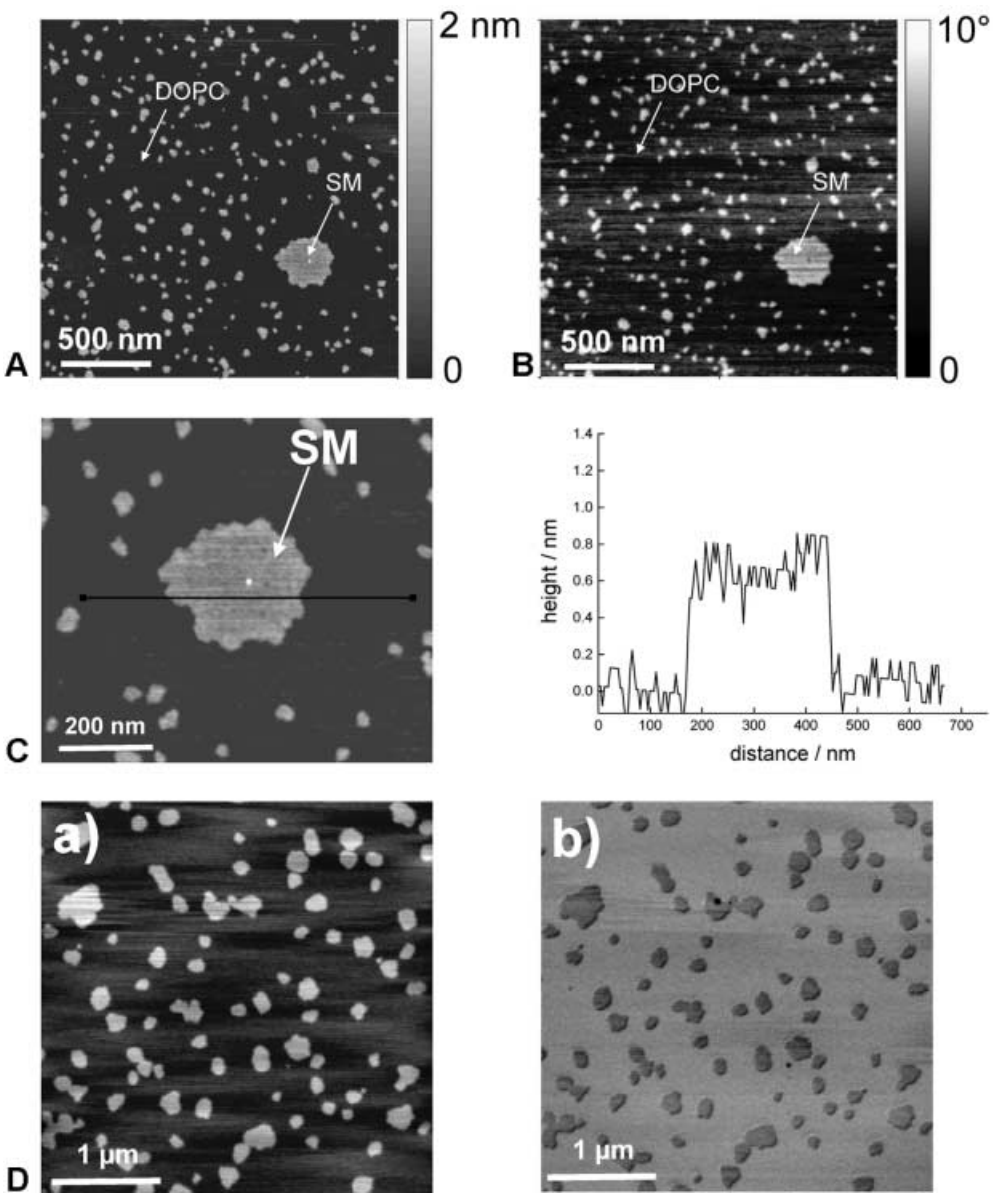

Fig. 1. **A** Topography image of a DOPC/SM (80:20) LB monolayer transferred at 36 mN/m to mica obtained by tapping mode AFM (2×2 µm). The amplitude was ca. 50–70 nm. **B** Phase contrast (phase angle shift between the free and interacting cantilever) of the corresponding image. **C** Height profile of SM domains in DOPC (image size 840×780 nm, *z*-scale 2 nm). The height difference between the DOPC and SM phase is approximately 0.7 nm. **D** Force modulation microscopy of a POPC/SM monolayer transferred to mica at 36 mN/m (3.6×3.6 µm). The amplitude was ca. 4–8 nm. **a** Topography (*z*-scale 3.3 nm). **b** Amplitude of the cantilever oscillation (*z*-scale 0.3 V photodiode signal) displaying the elasticity of the membrane leaflet. *Bright colors* refer to softer material

differences in elasticity rather than on variations in contact area (Magonov et al. 1997). Accordingly, we found that choosing a smaller amplitude ratio than 0.3 results in contrast inversion, which supports the assumption that contact area dominates the contrast-forming mechanism at severe tapping conditions, while at moderate tapping, elasticity differences govern image contrast. Bright colors refer to a more positive phase shift.

The height difference between the LC phase (SM) and the LE phase (DOPC) is 0.8 ± 0.1 nm, as obtained from histogram analysis (data not shown). For POPC/SM we found a height difference between the SM domains and POPC of 0.9 ± 0.1 nm. Figure 1C shows a typical line profile with a height difference of 0.7 nm. The lateral size of the LC domains is about 30–90 nm on average, although sometimes larger domains have been observed. The area occupied by the LC phase with respect to the LE phase corresponds to the initial ratio of POPC or DOPC to SM of 80:20. DOPC and POPC as the fluid components gave essentially the same results. Notably, the height difference depends on the imaging mode. The tapping mode gave slightly smaller height differences than the contact mode, while force modulation provides the largest difference in height, which is probably due to different indentation depths of the three methods.

Force modulation microscopy (FMM) provides an excellent means to probe for viscoelasticity differences (Jourdan et al. 1999). Figure 1D shows the topography and amplitude in force modulation mode imaging a POPC/SM (80:20) monolayer on mica. The amplitude of the cantilever oscillation forced by a piezo bimorph at approximately 8 kHz is lower (dark) on the higher LC domains (SM phase), as expected from the fact that the amplitude of a cantilever oscillation is larger for a softer material, i.e. the POPC matrix, since the soft material can be significantly penetrated.

Monolayers of POPC/SM (80:20) or DOPC/SM (80:20) with a small amount of G_{M1} (0.2 mol%) show the occurrence of an additional phase within the LC domains of the SM-enriched phase, indicated by an increase in height (1.0 ± 0.1 nm) with respect to the SM phase as shown in Fig. 2. The increase in height might be attributed to the bulkier headgroup of the gangliosides; thus the glycolipid consumes more space vertically as well as laterally. The fluid matrix of DOPC or POPC shows no change in topography. Small SM domains (LC phase, 30 nm in diameter) exhibit a G_{M1}-containing phase exactly in the center of the domain, which occupies about 1/4 of the overall area of the LC domain (Fig. S1 in the Supplementary material). This additional phase solely occurs in the ordered SM phase and displays a homogeneous height distribution. Owing to the matching chain length and structure of SM and G_{M1}, it seems reasonable that G_{M1} solely partitions into the LC domains formed by SM. Figure 2B shows a situation in which several LC domains merged to a larger micrometer-sized domain. As a consequence, the increased local concentration of the G_{M1}-enriched phase induced the formation of significant protrusion of more than 5–7 nm into the subphase (insert of Fig. 2B). This process is probably the initialization of micellization of G_{M1} into the water phase. The inner structure of the large domains shows a network of SM filamentous domains with small G_{M1}-enriched domains on top of the LC domains. The network-like structure is probably the result of coalescence of LC domains, as described by Yuan and Johnston (2000) for DPPC/G_{M1}. Notably, the G_{M1}-enriched phase is always located in the center of the SM (LC) domains. This finding is in contrast to the observation of Yuan and Johnston (2000) and Vie et al. (1998), who reported that G_{M1} is located mainly at the border of the LC domains of DPPC in the two-phase region. However, the authors used DPPC instead of SM, which may account for the differences since the affinity of G_{M1} for SM may be higher than for DPPC, which explains the preferential partition of the G_{M1}-enriched phase in the center of the SM domains.

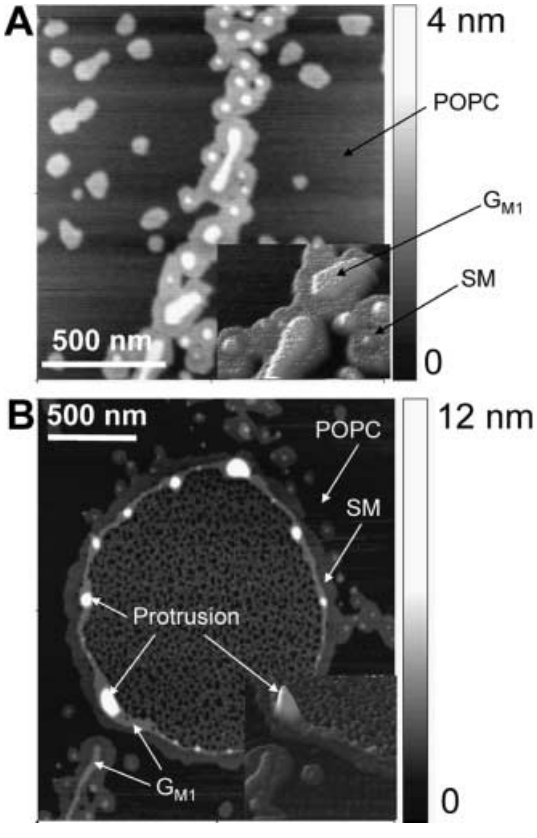

Fig. 2. **A** Topography of POPC/SM (80:20) monolayer with 0.2 mol% G_{M1} imaged by tapping mode AFM (1.4×1.4 μm). The *inset* is a magnification displayed in a three-dimensional view. The G_{M1}-enriched phase is 1.0 ± 0.1 nm higher than the SM phase. **B** Different location of the same film showing protrusions of G_{M1}-enriched material (*arrow*) of 5–7 nm budding into the subphase (2×2 μm). The *inset* is a magnification of the G_{M1}-enriched protrusion displayed in a three-dimensional view

SFM provides the possibility to extend the study of lipid monolayers towards material properties such as elasticity and adhesion. Force modulation images of POPC/SM/G_{M1} monolayers on mica transferred at 36 mN/m show the same contrast as the image shown in Fig. 1D. The G_{M1}-enriched phase exhibits the same stiffness as the surrounding SM phase, indicative of an ordered lipid matrix. These findings are supported by phase imaging, which shows essentially no contrast between the G_{M1}-containing lipid phase and the SM mother domains. Adhesion mapping by the pulsed force mode also confirms that the nature of the highest phase is identical to that of the SM domains (Fig. S2 in the Supplementary material). PFM shows essentially no difference in adhesion between the SM and G_{M1} phases. The LC domains, however, exhibit significant smaller adhesion between the tip and sample than on the POPC matrix, which is probably due to the reduced contact area on the stiffer material. This way, adhesion contrast reflects stiffness contrast.

Although SFM is not the best tool to perform statistics on a wider area, it is obvious that the higher domains do not consist solely of G_{M1} but of a mixture of SM and G_{M1}. This is in accordance with the findings of Yuan and Johnston (2000), who observed a similar behavior for mixed monolayers of G_{M1} and DPPC. The reason lies presumably in the fact that G_{M1} is negatively charged, thus avoiding close clustering due to electrostatic repulsion.

In order to answer the question of how cholesterol would affect the phase behavior of a phase-separated monolayer, we used a mixture of POPC/SM/Chol (2:1:1), which has been reported to form a heterogeneous phase composed of the liquid disordered phase l_d and liquid ordered phase l_o in bilayer systems (Brown and London 2000). Le Grimellec and co-workers already provided an excellent study investigating the influence of cholesterol on the phase behavior of mixed monolayers containing SM and POPC as the fluid component (Milhiet et al. 2001). Therefore, we focused on the phase

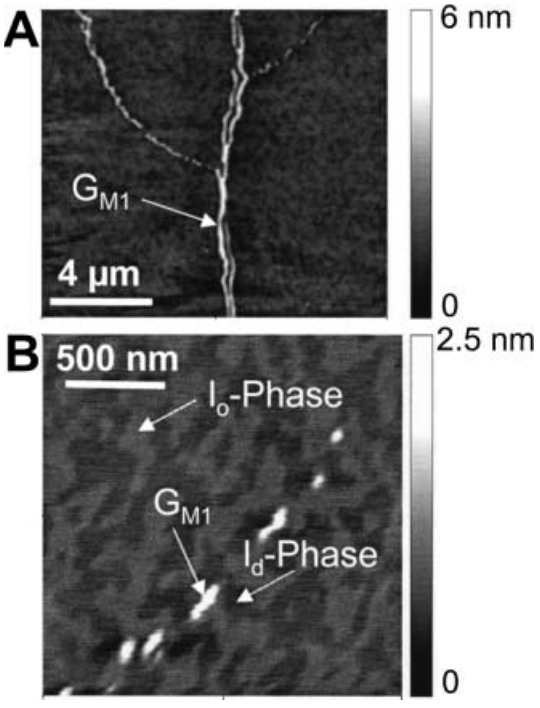

Fig. 3. **A** Tapping mode image of a POPC/SM/Chol (2:1:1) monolayer with 0.2 mol% G_{M1} transferred at 36 mN/m to mica (13×12 µm). **B** A POPC/SM/Chol (2:1:1) monolayer with 0.2 mol% G_{M1} imaged at higher magnification (image size: 1.8×1.8 nm), revealing the coexistence of ordered and disordered phases corresponding to the l_o and l_d phases in bilayers systems. The height difference is about 0.4 ± 0.1 nm. G_{M1} is solely found associated with the ordered phase (*arrow*)

behavior of G_{M1} in such a raft-forming mixture (l_o phase). Figure 3 shows the influence of cholesterol on the distribution of G_{M1}. Apparently, the presence of cholesterol did not abolish the occurrence of phase separation as expected from phase diagrams, which predict a coexistence of a disordered and an ordered phase. We found, in accordance with the study of Le Grimellec, that cholesterol increases the area occupied by the SM-enriched phase. The ordered phase consumes almost twice the area as anticipated from the initial composition. In accordance with the findings of Le Grimellec, we can still observe a SM-enriched phase coexistent with a liquid-like POPC-enriched phase. However, image contrast based on topography is reduced, which may be attributed to the presence of cholesterol in the SM and the POPC phases, thus reducing the usual height difference of the two phases (0.2 ± 0.2 nm instead of 0.8–0.9 nm). This can be explained in terms of a preferential interaction of cholesterol with SM as shown by Demel et al. (1977) and Slotte (1999), presumably due to the interaction of the hydroxyl group of cholesterol with the hydration shell of the SM headgroups.

Most strikingly, the G_{M1}-enriched phase displaying the greatest height is still present in the SFM images (Fig. 3) and G_{M1} clusters can be observed. However, the number of G_{M1}-enriched domains is reduced as compared to cholesterol-free monolayers. Omitting SM and using a monolayer consisting of POPC/Chol (70:30) with 0.2 mol% G_{M1} results in the occurrence of very few small domains (80–100 nm) with a height of approximately 0.7 nm, indicative of G_{M1} clusters. A monolayer of POPC/Chol in the absence of SM and G_{M1} is featureless, as predicted by McConnell (Radhakrishnan and McConnell 1999, 2000).

Notably, lateral organization at the air-water interface may be different from the monolayers that were transferred to the solid substrate. However, it was shown previously that domain organization of phopholipids is preserved on a micrometer scale while transferring the film from the air-water interface to a solid substrate (Galla et al. 1998). However, there is still uncertainty on a nanometer scale.

Conclusions

SFM is a powerful tool to probe phase behavior of lipid mono- and bilayers with nanometer resolution. The paper shows that G_{M1}, a prominent receptor lipid for toxins, lectins, viruses, and a marker for rafts occurring in the outer leaflets of cells, is distributed preferentially within the ordered matrix of the LC phase. Material contrast images show that the G_{M1}-enriched domains exhibit the same material properties as the host matrix represented by the LC domains. This behavior is preserved even after addition of cholesterol that is known to disperse phase boundaries. Furthermore, the occurrence of three-dimensional protrusion originating from the G_{M1}-enriched phase could be observed. From these results it is reasonable to conclude that clustering of ceramide-based glycolipids in the outer leaflet of biological membranes is very likely to play a pivotal role in ligand recognition and membrane organization. Consequently, the investigation of native membranes by scanning probe techniques remains a task for future investigations to gather more information on the structure-function relationships of biological membranes.

References

Brown DA, London E (1998a) Structure and origin of ordered lipid domains in biological membranes. J Membr Biol 164:103–114

Brown DA, London E (1998b) Functions of lipid rafts in biological membranes. Annu Rev Cell Dev Biol 14:111–136

Brown DA, London E (2000) Structure and function of sphingolipid- and cholesterol-rich membrane rafts. J Biol Chem 275:17221–17224

Demel RA, Jansen J, van Dieck P, van Deenen LLM (1977) The preferential interaction of cholesterol with different classes of phospholipids. Biochim Biophys Acta 465:1–10

Dietrich C, Bagatolli LA, Volovyk ZN, Thompson NL, Levi M, Jacobsen K, Gratton E (2001) Lipid rafts reconstituted in model membranes. Biophys J 80:1417–1428

Dufrene YF, Lee GU (2000) Advances in the characterization of supported lipid films with the atomic force microscope. Biochim Biophys Acta 1509:14–41

Fishman P, Brady R (1976) Biosynthesis and function of gangliosides. Science 194:906–915
Fivaz M, Abrami L, van der Goot F (2000) Pathogens, toxins, and lipid rafts. Protoplasma 212:8–14
Galla HJ, Bourdos N, von Nahmen A, Sieber M (1998) The role of pulmonary surfactant protein C during the breathing cycle. Thin Solid Films 327–329:632–635
Habermann E, Dreyer F (1986) Clostridial neurotoxins: handling and action at the cellular and molecular level. Curr Topics Microbiol Immunol 129:94–197
Hakomori S (1981) Glycosphingolipids in cellular interaction, differentiation, and oncogenesis. Annu Rev Biochem 50:733–764
Holmgren J, Elwing H, Fredman P, Svennerholm L (1980) Polystyrene-adsorbed gangliosides for investigation of the structure of the tetanustoxin receptor. Eur J Biochem 106:371–379
Janshoff A, Steinem C, Sieber M, Galla H-J (1996) Specific binding of peanut agglutinin to GM1 doped solid supported lipid bilayers investigated by shear wave resonator measurements. Eur Biophys J 25:105–113
Janshoff A, Steinem C, Sieber M, el Bâya A, Schmidt MA, Galla HJ (1997) Quartz crystal microbalance investigation of the interaction of bacterial toxins with gangliosides containing solid supported lipid membranes. Eur Biophys J 26:261–270
Jourdan JS, Cruchon-Dupeyrat SJ, Huan Y, Kuo PK, Lin GY (1999) Imaging nanoscopic elasticity of thin film materials by atomic force microscopy: effects of force modulation frequency and amplitude. Langmuir 15:6495–6504
Magonov SN, Elings V, Whangbo MH (1997) Phase imaging and stiffness in tapping-mode atomic force microscopy. Surf Sci 375:L385–L391
Milhiet PE, Domec C, Giocondi MC, Van Mau N, Heitz F, Le Grimellec C (2001) Domain formation in models of the renal brush border membrane outer leaflet. Biophys J 81:547–555
Mou J, Yang J, Shao Z (1995) Atomic force microscopy of cholera toxin B-oligomers bound to bilayers of biological relevant lipids. J Mol Biol 248:507–512
Radhakrishnan A, McConnell HM (1999) Condensed complexes of cholesterol and phospholipids. Biophys J 77:1507–1517
Radhakrishnan A, McConnell HM (2000) Condensed complexes, rafts, and the chemical activity of cholesterol in membranes. Proc Natl Acad Sci USA 97:12422–12427
Rosa-Zeiser A, Weilandt E, Hild S, Marti O (1997) The simultaneous measurement of elastic, electrostatic and adhesive properties by scanning force microscopy: pulsed-force mode operation. Meas Sci Technol 8:1333–1338
Ross M, Steinem C, Galla HJ, Janshoff A (2001) Visualization of chemical and physical properties of calcium-induced domains in DPPC/DPPS Langmuir-Blodgett layers. Langmuir 17:2437–2445
Simons K, Ikonen E (1997) Functional rafts in cell membranes. Nature 387:569–572
Singh AK, Harrison SH, Schoeninger JS (2000) Gangliosides as receptors for biological toxins: development of sensitive fluoroimmunoassays using ganglioside-bearing liposomes. Anal Chem 72:6019–6024
Slotte JP (1999) Sphingomyelin-cholesterol interaction in biological and model membranes. Chem Phys Lipids 102:13–27
Tamm LK, Böhm C, Yang J, Shao Z, Hwang J, Edidin M, Betzig E (1996) Nanostructure of supported phospholipid monolayers and bilayers by scanning probe microscopy. Thin Solid Films 284–285:813–816
Vie V, Van Mau N, Lesnniewska E, Goudonnet JP, Heitz F, Le Grimellec C (1998) Distribution of gangliosides GM1 between two-component, two-phase phosphatidylcholine monolayers. Langmuir 14:4574–4583
Vyas KA, Patel HV, Vyas AA, Schnaar RL (2001) Segregation of gangliosides GM1 and GD3 on cell membranes, isolated membrane rafts, and defined supported lipid monolayers. Biol Chem 382:241–250
Yuan C, Johnston LJ (2000) Distribution of gangliosides GM1 in l-α-dipalmitoylphosphatidylcholine/cholesterol monolayers: a model for lipid rafts. Biophys J 79:2768–2781
Yuan C, Johnston LJ (2001) Atomic force microscopy studies of ganglioside GM1 domains in phosphatidylcholine and phosphatidylcholine/cholesterol bilayers. Biophys J 81:1059–1069